FULL PAPER

ADVANCED FUNCTIONAL MATERIALS

DOI: 10.1002/adfm.200700713

Modeling Electron and Hole Transport in Fluoroarene-Oligothiopene Semiconductors: Investigation of Geometric and Electronic Structure Properties**

By *Sharon E. Koh*, *Chad Risko*, *Demetrio A. da Silva Filho*, *Ohyun Kwon*, *Antonio Facchetti*, *Jean-Luc Brédas*,* *Tobin J. Marks*,* and *Mark A. Ratner**

A theoretical study using density functional theory is undertaken to gain insight into how the structural, electronic, and electron-transfer characteristics of three Fluoroarene-oligothiophene semiconductors influence the preferred transport of electrons versus holes in field-effect transistor applications. The intermolecular electronic coupling interactions are analyzed through both a simplified energy-splitting in dimer (ESID) model and as a function of the entire dimer Hamiltonian in order to understand the impact of site energy differences; our results indicate that these differences are generally negligible for the series and, hence, use of the ESID model is valid. In addition, we also investigate the reduction and oxidation processes to understand the magnitudes of the intramolecular reorganization energy for the charge-hopping process and expected barrier heights for electron and hole injection into these materials. From the electronic coupling and intramolecular reorganization energies, estimates of the nearest-neighbor electron-transfer hopping rate constant for electrons are obtained. The ionization energetics suggest favored electron injection for the system with perfluoroarene groups at the end of the thiophene core, in agreement with experiments. The combined analyses of the electron-transfer properties and ionization processes suggest possible ambipolar behavior for these materials under favorable device conditions.

1. Introduction

π-Conjugated molecular, oligomeric, and polymeric materials are of immense interest as alternatives to traditional inorganic materials for many low-cost organic-based electronics applications–including thin-film transistors (OTFTs),[1–6] light-emitting diodes (OLEDs),[7–14] and photovoltaic cells[15–17] –owing to device processing ease, mechanical flexibility, and a large synthetic palette from which properties can be designed into the molecular or polymeric structures.[18–20] However, many fundamental questions concerning how charge is transported through these functional organic molecular solids remain unresolved. In particular, why certain molecular materials favor the transport of holes versus electrons (i.e., positive and negative polarons, respectively) and how molecular and crystal structure parameters influence relative carrier mobility magnitudes are far from being completely understood.[21–23]

In typical organic transport media, very small bandwidths (< 1 eV) dictate that charge motion occurs by hopping. The electron-hopping process is generally portrayed as a self-exchange electron-transfer reaction between neighboring molecules within the framework of Marcus theory and extensions thereof.[22,24–27] The rate constant for electron transfer (i.e., polaron hopping) is then defined in an Arrhenius-like form:

$$k_{ET} = \frac{4\pi}{h}\frac{1}{\sqrt{4\pi\lambda k_B T}} t_{12}^2 \exp\left[\frac{-\lambda}{4k_B T}\right] \quad (1)$$

where λ is the reorganization energy for the intermolecular electron transfer, t_{12} is the electronic coupling element (transfer integral) between neighboring molecules, h is Planck's constant, k_B is the Boltzmann constant, and T is the temperature. The reorganization energy λ can be separated into the sum of two primary components: i) the medium reorganization energy (i.e., outer-sphere reorganization energy, λ_0) that arises from modifications to the medium polarization due to the presence of an excess charge; and ii) the intramolecular reorganization energy (i.e., inner-sphere reorganization energy, λ_i) that provides a measure of the intramolecular electron-vibration inter-

[*] Prof. T. J. Marks, Prof. M. A. Ratner, Dr. S. E. Koh, Dr. C. Risko, Dr. A. Facchetti
Department of Chemistry and Materials Research Center
Northwestern University
Evanston, IL 60208 (USA)
E-mail: t-marks@northwestern.edu; ratner@northwestern.edu
Prof. J.-L. Brédas, Dr. D. A. da Silva Filho, Dr. O. Kwon[+]
School of Chemistry and Biochemistry and
Center for Organic Photonics and Electronics (COPE)
Georgia Institute of Technology
Atlanta, GA 30332 (USA)
E-mail: jean-luc.bredas@chemistry.gatech.edu
[+] Current Address: Samsung Advanced Institute of Technology Mt. 14-1, Nongseo-Dong, Giheung-Gu, Yongin-Si Gyunggi-Do, 446-712, Korea.

[**] The authors would like to thank the Office of Naval Research (N00014-02-1-0909 & N00014-04-0120) and the NSF under the MRSEC program (DMR-0520513 & DMR-0212302) and under the CRIF (CHE-0443564) for funding this project. Supporting Information is available online from Wiley InterScience or from the authors.

ADVANCED FUNCTIONAL MATERIALS

action for the sequential reduction and oxidation processes of polaron hopping. Along with the original dielectric continuum model put forth by Marcus, numerous explorations into expressions to describe λ_0 are currently ongoing.[24–26,28–32] λ_i can be determined quantum-chemically from the individual relaxation process energies for the neighboring electron-donor and electron-acceptor species; as an example, λ_i for the reduction of an electron-acceptor (neutral species, λ_1) via oxidation of a doublet electron-donor (radical-anion, λ_2), see Figure 1, can be obtained by the expression shown in Equation 2:

$$\lambda_i = \lambda_1 + \lambda_2 = \left(E_0^{-1} - E_0^0\right) + \left(E_{-1}^0 - E_{-1}^{-1}\right) \tag{2}$$

where λ_i is the total intramolecular reorganization energy and λ_1 [λ_2] is the reorganization energy of the electron-acceptor [electron-donor].

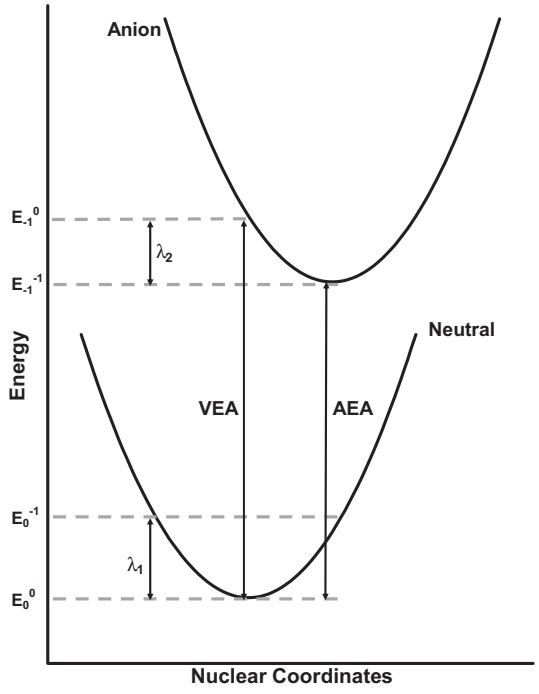

Figure 1. Energy diagram of ionization processes.

Following the work of Siebbeles et al.[33,34] and Coropceanu et al.[35,36], the electronic Hamiltonian of a simple two-site (i.e., dimer pair) tight-binding model[37] can be written as

$$\hat{H} = \begin{pmatrix} e_1 & t_{12} \\ t_{21} & e_2 \end{pmatrix} \tag{3}$$

The electronic coupling (transfer integral) is defined by the matrix element $t_{12} = t_{21} = \left\langle \Psi_1 \middle| \hat{H} \middle| \Psi_2 \right\rangle$, where Ψ_1 and Ψ_2 are diabatic state wave functions for neighboring molecules. Within the one-electron approximation, the diabatic states are associated with localized monomer orbitals φ_i, here considered to be orthogonal. Assuming that the dimer highest-occupied molecular orbital (HOMO) [lowest-unoccupied molecular orbital (LUMO)] and HOMO-1 [LUMO+1] result solely from the interaction of the monomer HOMOs [LUMOs], the transfer integral for hole (Eq. 4a) [electron, Eq. 4b] transfer can be expressed as:

$$t_{12}^H = \left\langle \varphi_1^H \middle| \hat{H} \middle| \varphi_2^H \right\rangle \tag{4a}$$

$$t_{12}^H = \left\langle \varphi_1^L \middle| \hat{H} \middle| \varphi_2^L \right\rangle \tag{4b}$$

The diagonal elements of this matrix are the site energies – which originate from differences in either molecular geometry or intermolecular polarization of localized electronic states – and are expressed as:

$$e_1 = \left\langle \varphi_1^{H[L]} \middle| \hat{H} \middle| \varphi_1^{H[L]} \right\rangle \tag{5a}$$

$$e_2 = \left\langle \varphi_2^{H[L]} \middle| \hat{H} \middle| \varphi_2^{H[L]} \right\rangle \tag{5b}$$

Solving the determinant of this matrix provides the relationship between the transfer integral, site energy, and expected degree of energetic splitting of the dimer molecular orbitals (ΔE_{12}) via

$$\Delta E_{12} = \sqrt{(e_1 - e_2)^2 + (2t_{12})^2} \tag{6}$$

However, as stated above, the tight-binding approximation assumes an orthogonal basis and the Löwdin's symmetric transformation can be applied to a nonorthogonal basis to generate an orthonormal one that maintains as much as possible the initial local character of the monomer orbitals. Usually, in the one-electron approximation, the monomer orbitals used to define the diabatic states of the dimer are nonorthogonal. Therefore, ΔE_{12} in a nonorthogonal basis should be written as

$$\Delta E_{12} = \frac{\sqrt{(\tilde{\varepsilon}_2 - \tilde{\varepsilon}_1)^2 + 4\left(\tilde{t}_{12}^2 - \tilde{t}_{12} S_{12}(\tilde{\varepsilon}_2 + \tilde{\varepsilon}_1) + \tilde{\varepsilon}_2 \tilde{\varepsilon}_1 S_{12}^2\right)}}{1 - S_{12}^2} \tag{7}$$

where $\tilde{\varepsilon}_{12}$ and $\tilde{t}_{12}$ are the site energies and electronic coupling in the nonorthogonal basis and S_{12} is the spatial overlap between the molecular orbitals on the monomers.[36] Equation 6 is rewritten as Equation 7 in a symmetrically orthonormalized basis when

$$\varepsilon_{1(2)} = \frac{1}{2} \frac{(\tilde{\varepsilon}_1 + \tilde{\varepsilon}_2) - 2\tilde{t}_{12} S_{12} \pm (\tilde{\varepsilon}_1 - \tilde{\varepsilon}_2)\sqrt{1 - S_{12}^2}}{1 - S_{12}^2} \tag{8}$$

and

$$t_{12} = \frac{\tilde{t}_{12} - \frac{1}{2}(\tilde{\varepsilon}_1 + \tilde{\varepsilon}_2) S_{12}}{1 - S_{12}^2} \tag{9}$$

This full expression incorporating the overlap is utilized herein.

As with the reorganization energy, quantum-chemical calculations can provide access to estimates for the electronic coupling element. The most common means of estimating t_{12} is the energy-splitting in dimer (ESID) model.[37] Due to computational ease and feasibility, the transfer integral for hole [electron] transfer is generally taken as half the energetic difference of the HOMO and HOMO-1 [LUMO and LUMO+1] energy levels of a molecular dimer; the ESID model strictly implies that differences in the site energies given in Equations 5a and 5b are necessarily zero or negligible ($e_1 \cong e_2$). Recent work,[35,36] however, has indicated that this assumption is often invalid in organic crystalline semiconductors and, thus, t_{12} should be evaluated as a function of the entire dimer Hamiltonian (EDH).[33,35,36] As Equation 6 reveals, neglect of site energy inequality can lead to overestimations of the transfer integral. For example, along the diagonal direction of herringbone crystals (e.g., pentacene, when only one inequivalent molecule is present in the crystal structure), the molecular sites are equivalent as long as all the neighboring molecules are taken into account. However, when a dimer is extracted from the crystalline environment, the two herringbone-packed molecules are no longer equivalent and an artificially created site energy difference has to be properly taken into account to evaluate the electronic coupling.[36]

To date, most organic semiconductors have been found to be hole-channel charge transporters.[38–48] However, for diode-based applications, electron-channel organic conductors are important. Empirical evidence suggests that the addition of electron-withdrawing substituents to the core of the oligomer/polymer provide stronger electron affinities (often estimated from the LUMO). Fluorocarbon-oligothiophene isomers containing variously positioned perfluorinated-arene and alkyl substituents[3,4,49–51] are of particular interest as the thiophene-based semiconductors have stabilized LUMO energies in comparison to other heteroatom aromatics, as well as other favorable properties including chemical and thermal stability, synthetic tailorability, and relatively large carrier mobilities.[3,4,51–56] Indeed, substantial mobilities and n-type carrier dominance have been observed in these materials, a striking variance from the p-type transport typical of unfunctionalized and hydrocarbon-functionalized oligothiophenes.[48,52–55,57,58]

In this contribution, we focus on the structural, electronic, and transport properties of three electrically and crystallographically characterized mixed-polarity molecules with perfluoroarene groups sequentially located at different skeletal positions; each molecule contains six rings, two perfluoroarene units and four thiophene rings (see Fig. 2).[58] The archetypical p-type conductor **6T** is also investigated for comparison.[1,57] We are interested in detailing further how the placement of the perfluoroarene units affect the ionization processes and electronic coupling in these structurally analogous oligomeric systems, with the ultimate goal of understanding how these properties result in the observed differences in majority carrier sign and k_{ET}.

2. Results

2.1. Geometry

Selected geometric parameters for the optimized neutral, radical-anion, and radical-cation states of **6T**, **FTTTTF**, **TFTTFT**, and **TTFFTT** are listed in Tables S1–S8 in the Supporting Information (Fig. S1 provides the reference bond numbering scheme). The DFT calculated neutral states for **FTTTTF**, **TFTTFT**, **TTFFTT** are in good agreement with the crystal structures. Calculated structures with the B3LYP functional provided better agreement with crystal geometries versus PW91 and will be discussed in this section. Calculated dihedral angles measured from thiophene–thiophene (S–C–C–S) reveal a planar core for **FTTTTF** with φ_1 being 180°; however, the remainder of the molecule appears slightly twisted with φ_2 and φ_3 being 21.6° and 11.8° respectively (dihedral notation is given in Supporting Information). **TFTTFT** also possesses a relatively planar core as well as a fairly planar thiophene-phenyl interaction with φ_2 and φ_3 both having angles of 0.7°. For **TTFFTT**, the fluorinated-phenyl ring junction in the middle of the molecule provides a significant twist with a torsion of 52.6°;

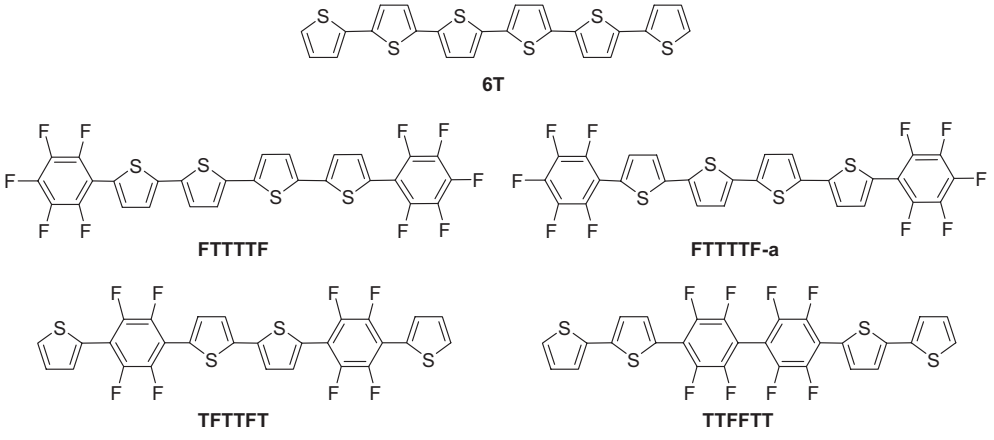

Figure 2. Molecular structures of perfluoroarene-modified oligothiophenes.

ADVANCED FUNCTIONAL MATERIALS

the thiophene–phenyl ring interaction appears planar (~ 0.6°) for φ_2, and the thiophene–thiophene interaction also seems to be relatively planar with $\varphi_3 = 176.8°$. All three fluoroarene compounds are more twisted compared to the planar **6T** structure. We note that **FTTTTF** shows a preferred *syn*-conformation between outer pairs of thiophene rings in the experimental crystal structure.[49,50] The DFT results, however, show that the *anti*-conformer is energetically stabilized by 1.6 kcal mol^{-1} versus the *syn*-conformer – an energetic difference that could be overcome by crystal packing effects and lead to the *syn*-conformer in the solid-state.

Reduction and oxidation of the four molecular systems bring about substantial bond-length alternation (BLA)[59] modification along the C–C backbone of the oligomeric structures. The BLA shifts for both reduction and oxidation in **6T** predominantly occur within the four central thiophene units; minimal changes occur for the two external thiophene rings; while there is nominal change in the S–C bond lengths for oxidation, the S–C bonds lengthen by 0.02 Å upon reduction. Similar geometric changes occur upon reduction and oxidation for both **FTTTTF** and **TFTTFT** – structures in which the central rings are thiophenes. The BLA in the C–C backbone of the central thiophene units alters significantly upon both reduction and oxidation, while the external thiophene ring in **TFTTFT** shows modest modifications; changes to the S–C bond lengths also show similar patterns for reduction and oxidation. The perfluoroarene units undergo relatively modest BLA changes compared to the thiophene units. For **TTFFTT**, with central perfluoroarene groups, the structural changes due to oxidation are predominately localized on the thiophene units. Reduction leads to more delocalized modifications to the geometry, including more significant changes in the perfluoroarene units and less change within the thiophene rings versus the other structures. Both radical-ion species for each system are more planar than the neutral, with **FTTTTF** showing the most pronounced difference between neutral and charged species.

2.2. Energetics of Ionization

Vertical and adiabatic ionization potentials and electron affinities are given in Table 1. Substitution of the perfluoroarene groups into **6T** stabilizes the radical-cation state on the order of 0.4–0.6 eV. The energetic stabilization of the radical-cation increases as the perfluoroarene units are moved towards the center of the oligomeric structure. Electron affinities reveal a similar energetic stabilization (ca. 0.1–0.3 eV) of the radical-anion state. However, the electron affinities are most energetically-stabilized when the perfluoroarenes are on the oligomer exterior.

From Equation 2 we determine the intramolecular contribution to the total reorganization energy (λ_i); the individual relaxation components and total intramolecular reorganization energies for reduction and oxidation are given in Table 1. The reorganization energies for both reduction and oxidation are on the order of 0.20–0.34 eV. The results for these inter-ring structures are two-to-three times larger than those for the fused-ring oligoacene structures (e.g., pentacene: 0.097 eV for oxidation and 0.130 eV for reduction).[60,61] The reorganization energies for each structure are similar for both reduction and oxidation – results in line with the similar geometric changes observed for both ionization processes. Amongst the structures, **6T**, **TFTTFT**, and **TTFFTT** have comparable reorganization energies, while those for **FTTTTF** are appreciably larger due to the significant planarization of the system (vide supra) induced by ionization.

Table 1. Vertical and adiabatic ionization potentials (VIP and AIP, respectively) and electron affinities (VEA and AEA, respectively), and the relaxation energies and total reorganization energies associated with the respective oxidation and reduction processes as determined at the B3LYP/6-31G** level. All energies are in eV.

	Oxidation					Reduction				
	VIP	AIP	λ_1	λ_2	λ_{ox}	VEA	AEA	λ_1	λ_2	λ_{red}
6T	5.86	5.75	0.13	0.12	0.25	–1.14	–1.25	0.11	0.11	0.22
FTTTTF	6.29	6.11	0.13	0.19	0.32	–1.36	–1.56	0.14	0.20	0.34
TFTTFT	6.38	6.27	0.12	0.11	0.23	–1.36	–1.48	0.12	0.12	0.24
TTFFTT	6.48	6.39	0.10	0.09	0.19	–1.24	–1.36	0.11	0.11	0.22

2.3. Electronic Coupling

Both the ESID and EDH models rely on information pertaining to the monomer electronic structure; therefore, HOMO and LUMO energies are given in Table 2 and pictorial representations of the monomer and dimer molecular orbitals are contained in Supporting Information. The trends in the HOMO and LUMO energies match those of the ionization potentials and electron affinities. The perfluoroarene units stabilize the HOMO versus **6T**, with the stabilization increasing as the perfluoroarene groups are moved towards the center of the oligomeric structures. The computed HOMO values are in good agreement with the experimentally derived ionization energy values extrapolated from thin-film electrochemistry;[49,50] electrochemically-measured redox potentials are often used as estimates to HOMO/LUMO energies by adding 4.4 eV from the E_{onset} to obtain ionization potential (IP) or electron affinity (EA). [$E_{onset}^{oxidation}$ = IP – 4.4; and for $E_{onset}^{reduction}$ = EA – 4.4].[54,62–65] The LUMO energies, likewise, are stabilized versus **6T** with perfluoroarene substitution; however, the LUMO is more energetically stabilized with the perfluoroar-

Table 2. DFT-derived and Experimentally-Estimated HOMO and LUMO Energies (eV) at the B3LYP/6-31G** [58] and PW91/6-31G**.

	B3LYP/6-31G**		PW91/6-31G**		Exp. [a]	
	HOMO	LUMO	HOMO	LUMO	HOMO	LUMO
6T	–4.79	–2.20	–3.05	–1.71	–5.20 (–4.78)	–2.65 (–2.36)
FTTTTF	–5.20	–2.39	–3.44	–1.87	–5.48 (–5.27)	–2.85 (–2.69)
TFTTFT	–5.33	–2.39	–3.56	–1.85	–5.64 (–5.32)	–2.82 (–2.67)
TTFFTT	–5.47	–2.29	–3.71	–1.70	–5.81 (–5.40)	–2.81 (–2.53)

[a] Electrochemical redox values were obtained both in THF and thin-film (parentheses) measurements.

enes on the exterior. The molecular orbital density distributions have been described previously.[58] The majority of the molecular orbital density in both the HOMO and LUMO resides on the C-C backbone. Contributions from the sulfur atoms are found to contribute predominantly in the LUMO, while the fluorine atoms act chiefly through inductive effects.

Previous estimates[58] of t_{12} for these materials have been made with the ESID method using the B3LYP functional with atomic positions taken directly from the corresponding crystal geometry. The results, along with estimations using the PW91 functional to compare with the full EDH calculations (vide infra), are given in Table 3. The B3LYP and PW91 ESID calculations are in good agreement. These results reveal that the electron and hole transfer integrals for **6T** are significantly larger than any of the perfluoroarene-thiophene systems. For hole transport, t_{12} is estimated to be approximately equal for **FTTTTF** and **TTFFTT** with **TFTTFT** being smaller; t_{12} for electron transport, on the other hand, is significantly larger for **TFTTFT** versus the other two species. We note, however, that **FTTTTF** and **TTFFTT** have slipped oligomer stacking that produces overlap interactions over only half of the molecule; a condition that can lead to a significant drop in the calculated t_{12}.

Table 3. Electronic coupling for hole and electron transport from the ESID model at the B3LYP/6-31G** and PW91/TZP levels of theory and the EDH model. All energies are in eV.

	ESID				EDH	
	B3LYP		PW91		PW91	
	Hole	Electron	Hole	Electron	Hole	Electron
6T	0.135	0.132	0.133	0.129	–	–
FTTTTF	0.057	0.011	0.056	0.017	0.053 [a]	0.030[a]
TFTTFT	0.034	0.069	0.033	0.062	0.026	0.062
TTFFTT	0.051	0.020	0.052	0.015	0.034	0.013

[a] Note that these values are obtained along different crystal vectors, but represent the largest electronic coupling observed in this system.

The EDH calculations were performed within the experimentally found crystal cell parameters for a collection of dimers; those listed herein provided the largest degree of electronic coupling and, hence, the most likely 'conduction pathways' for electron-transport through the crystal. **FTTTTF** has strongly interacting dimers along more than one direction. In particular, three sets of dimers were found to have reasonably large electronic couplings for both holes and electrons: a) 9 meV holes and 27 meV electrons; b) –13 meV holes and 30 meV for electrons; and c) 53 meV holes and –9 meV electrons (see Fig. 3a–c for for the dimer interaction geometries). For **TFTTFT**, only one dimer has non-negligible hole or electron coupling. Along the **b** crystallographic axis, the slipped cofacial arrangement with an interplane distance of ca. 3.5 Å (measured using the central bithiophene) produced hole and electron couplings of 26 meV and 62 meV, respectively; the 62 meV coupling for electrons was the largest for this series of three fluorinated molecules (Fig. 4). **TTFFTT**, as well, has only one dimer with non-negligible electronic coupling, with the

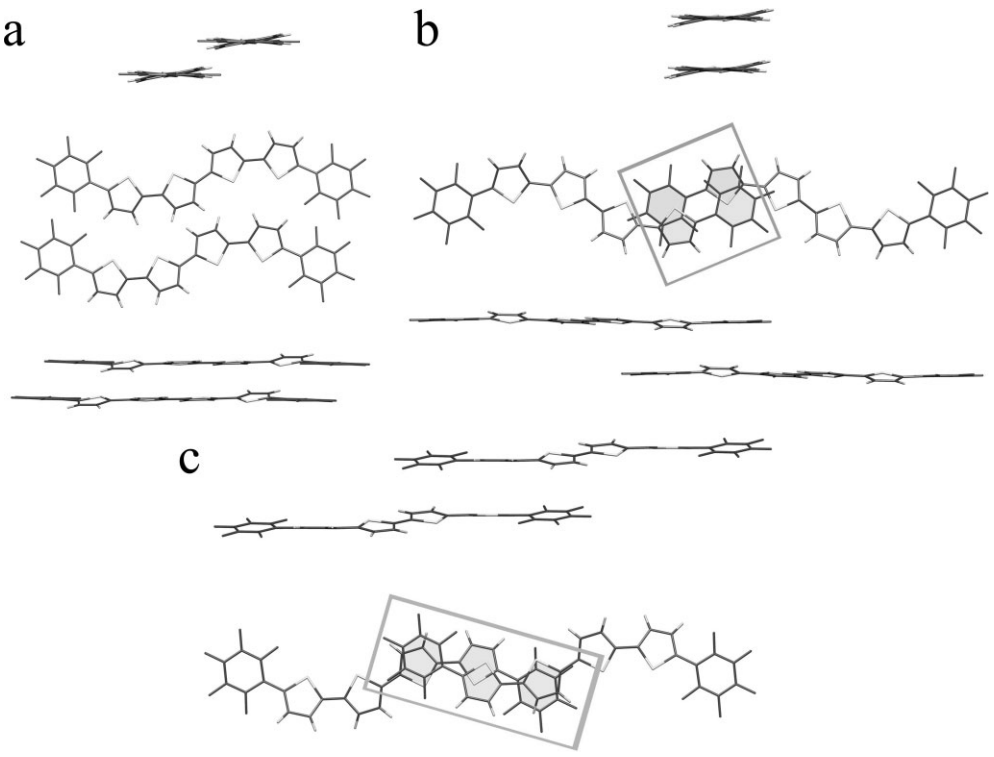

Figure 3. Dimer interactions for **FTTTTF** along different crystal axes with a) couplings of 9 meV for holes and 27 meV for electrons; b) couplings of –13 meV for holes and 30 meV for electrons c) couplings of 53 meV for holes and 9 meV for electrons. EDH method used. (Note that the sign of the electronic coupling arises from the symmetry of the orbitals.)

ADVANCED FUNCTIONAL MATERIALS

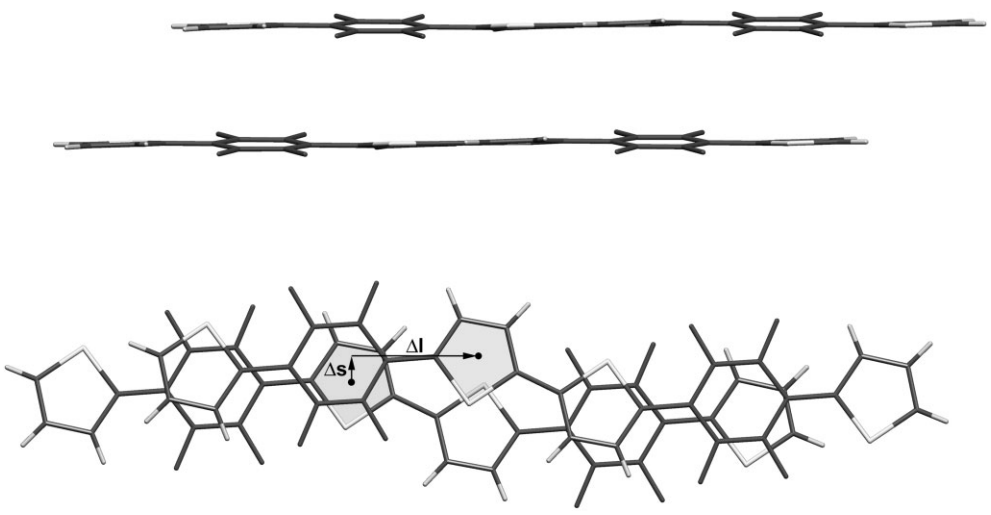

Figure 4. Dimer interactions along the *b*-crystal-axis for **TFTTFT** (EDH method) resulting in couplings of 26 meV for the holes and 63 meV for electons.

hole and electron couplings found to be –34 meV and 13 meV, respectively (Fig. 5). We note that the sign of the electronic coupling arises from the phase of the orbitals and has no impact on the evaluation of k_{ET}.

From the EDH theoretical parameters calculated above, estimates for k_{ET} using Equation 1 were made as a function of outer-sphere reorganization energy, see Figure 6. Although there are reported values for the outer-sphere reorganization energy in solution, this quantity cannot be easily estimated for charge-transport processes in solid state media. Previous theoretical studies have indicated that the outer-sphere reorganization energy could have the same order of magnitude of the intra-molecular reorganization energy.[22] Here, we have taken λ_0 as a variable parameter ranging from 0.03–0.6 eV, ca. $0.1\times$ – $2\times$ the inner-sphere reorganization energy. As expected, there is a strong dependence of the rate constant on the outer-sphere reorganization energy (ca. 2–3 orders of magnitude). The electron transport trends are determined to follow as **TFTTFT** > **FTTTTF** > **TTFFTT**, while the hole transport trends are predicted to be **TTFFTT** > **FTTTTF** > **TFTTFT.**

3. Discussion

In general, the electronic coupling results for the ESID and EDH models show negligible differences (~ 1 meV) for these oligomeric species. Therefore, it is apparent that site energies are of minimal consequence in these systems and that the assumptions made under the ESID model are reasonable. There are two exceptions, however, to these trends in the series: the electronic coupling for electrons in **FTTTTF** is predicted to be 1.8x larger in the EDH model versus the ESID model; and, the hole electronic coupling of **TTFFTT** is 1.5x smaller in the EDH model. These results indicate two important limitations of the calculations. First, by computing the two sides of Equation 6 independently (i.e., the left side from the orbital energy difference and the right side using the matrix elements e_1, e_2 and t_{12},) we can estimate that the numerical errors within the calculation are on the order of few meV. Second, and more importantly, there are instances in which other monomer molecular orbitals may contribute to the dimer molecular orbitals for which t_{12} is being evaluated;[66] recall Equation 3 relates t_{12} to only single orbitals,

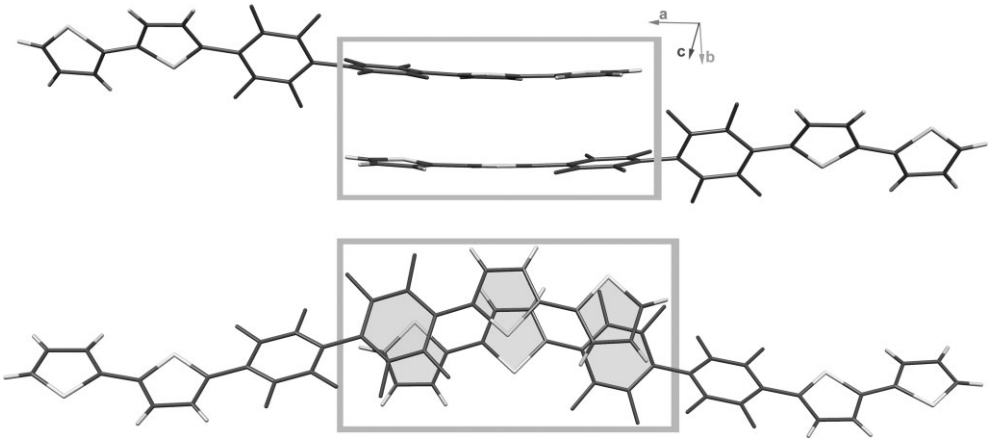

Figure 5. Dimer interactions for **TTFFTT** (EDH method) resulting in couplings of –34 meV for the holes and 13 meV for electons.

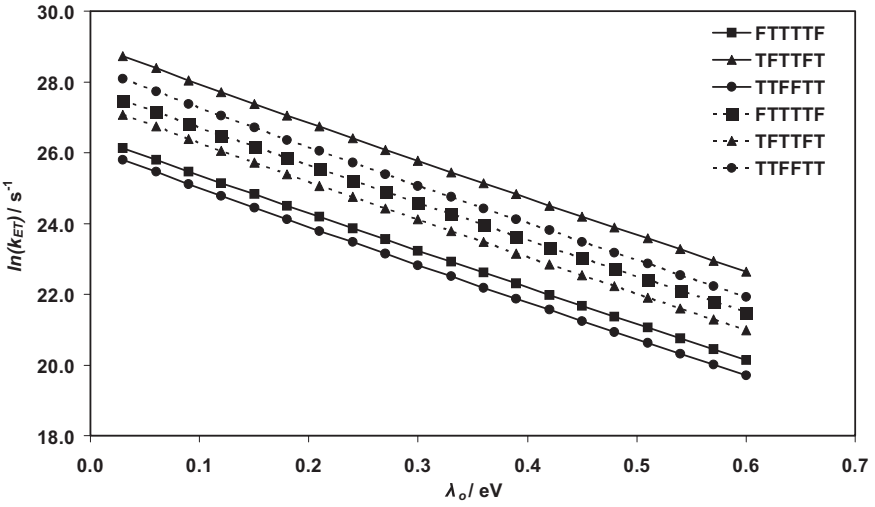

Figure 6. Estimated nearest neighbor electron-transfer rate constant (s^{-1}) for electron (solid line) and hole (dashed line) transport as a function of solvent (outer-sphere) reorganization energy.

not linear combinations of orbitals, on each molecular unit in the dimer. For example, there is considerable contribution (~ 20 %) from the monomer HOMO-1 of **TTFFTT** in the dimer HOMO. Therefore, such limitations need to be taken into account when evaluating t_{12} within the EDH model. For all calculations, the perfluoroarene-thiophene oligomers have a smaller electronic coupling (for both holes and electrons) compared to **6T**.

As a comparison to the crystal structure dimer, further analysis through the ESID model was performed with a perfect cofacial dimer model at a spacing of 3.20 Å for **FTTTTF**, 3.40 Å for **TFTTFT**, and 3.36 Å for **TTFFTT** see Figure 7. In the cofacial arrangement, there is a substantially larger HOMO and HOMO-1 [LUMO and LUMO+1] splitting versus the crystal dimer model (see Supporting Information for energy values). So, if these materials could be designed to pack in such a manner, large bands would be evident and higher hole and electron mobilities may be expected.

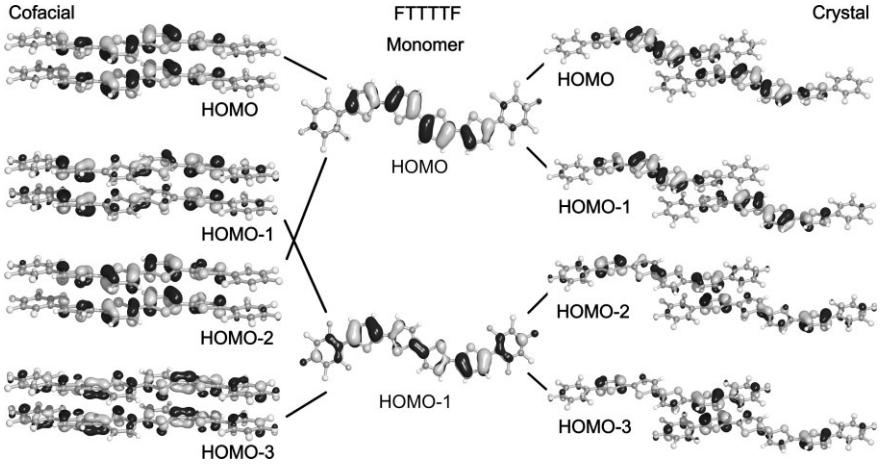

Figure 7. Pictorial representations of the **FTTTTF** monomer HOMO and HOMO-1 and crystal and cofacial (π–π stacking distance 3.2 Å) dimer HOMO through HOMO-3.

An additional factor besides the intermolecular electron-transfer parameters (λ_i and k_{ET}) that may affect overall device performance is the barrier for hole [electron] injection from the electrode. The injection barrier is often crudely estimated as the energetic difference between the ionization potential [electron affinity] and the Fermi energy of the source electrode (E_f(Au) = 5.2 eV).[67,68] The calculated vertical ionization potentials then would indicate that hole injection should be significantly easier for **6T** versus the perfluoroarene compounds, with hole injection barriers for the perfluoroarene compounds following **FTTTTF** < **TFTTFT** < **TTFFTT**. The opposite is the case for the electron injection where reduction of the perfluoroarene compounds is easier (**FTTTTF** $\geq$ **TFTTFT** > **TTFFTT**) than **6T**.

The question now arises: how does the interplay of these calculated parameters relate to the empirically-observed hole and electron mobilities? For electron transport, the calculated results seem to indicate that **TFTTFT** and **FTTTTF** could have similar mobilities measured in an OFET configuration: k_{ET} is greater for **TFTTFT**, but the system is charge-injection limited for FET mobility versus **FTTTTF**. Previous mobility measurements[49,50] reveal that **FTTTTF** has the largest overall mobility in this series; however, these larger mobility values were obtained for **FTTTTF** devices made at higher deposition temperatures (90 °C); with a thermal deposition temperature of 60 °C, **FTTTTF** and **TFTTFT** have similar charge carrier mobility values though opposite in charge polarity.[49,50] The results for hole transport are more obscure. Analysis of the various parameters for hole transport indicates that **FTTTTF** should exhibit the highest hole transport. However, the experimental results[49,50] show no measurable hole mobility for this system. This result, along with the changes in electron mobility upon differing deposition temperatures, points to a number of macroscopic device properties – including film morphology, dielectric polarizability, charge traps and interfacial variations – that we do not take into account in these theoretical analyses, but appear to have significant influence on the hole and electron mobilities of these systems. Further analyses of device structure, and how those properties affect the intrinsic transport properties, needs to be undertaken to understand fully their implications.

From the calculated electron-transfer parameters for holes and electrons, one might expect ambipolar transport properties for these materials under proper operating conditions. This is in agreement with

ADVANCED FUNCTIONAL MATERIALS

previously reported band structure analysis.[58] Thus, these materials should be ambipolar, with majority carrier depending on fabrication conditions. The concept of ambipolar behavior in organic semiconductors has been discussed by Sirringhaus and co-workers, who indicate that most organic systems should show both n- and p-type behavior under proper fabrication conditions.[69] Variations in these fabrication conditions may include monolayer treatments on the SiO_2 dielectric or changing the dielectric medium to induce preferred charge carriers.

4. Conclusions

We have presented a detailed theoretical analysis of the electron and hole transport properties of a series of perfluoroarene-thiophene oligomers. The results indicate that there is a delicate interplay between the calculated electron-transfer characteristics and charge-injection barriers that needs to be taken into account in the evaluation of such systems. The calculated data also suggest that macroscopic properties within the device architecture can overwhelm this balance and significantly alter the expected favored carrier mobilities. We expect these materials to act as ambipolar charge transporters under appropriate macroscopic conditions.

5. Experimental

Theoretical Methodology: Geometry optimizations of the neutral and radical-ion states were performed at the DFT level using the B3LYP hybrid functional [70,71] and a 6-31G** basis set. Analyses of the neutral and radical-ion states were also carried out with the PW91 functional [72,73]; the optimized geometries and electronic structures were found to be quite comparable for the two functionals. All isolated molecular calculations were performed with Q-Chem (version 2.1) [74].

The electronic coupling is a key parameter for the discussion of charge transport in both the hopping and band régimes. Herein, the electronic coupling in the hopping régime was evaluated directly as a matrix element with both the ESID and EDH models (vide supra). However, we note that the evaluation of the band structure followed by a tight-binding fitting offers a different means to compute the electronic coupling and should provide within the Marcus hopping picture similar results for the mobility compared to the direct evaluation of the matrix element. Once the band structure has been calculated, it is relevant to estimate the effective mass as there is a direct connection between this parameter and the mobility, since both, in a single tight-binding model, follow from the lattice constant and the tunneling integral; if the effective mass is compared directly to the mobility, one is indeed assuming band transport. The ESID and EDH calculations were performed assuming ideal conditions at 0 K to allow for comparison with previously calculated results for electronic coupling; recent work by A. Troisi [75] to develop a temperature-dependent phenomenological transport model has pointed to the importance of temperature on the electronic coupling – the disturbance of molecular structure and position via vibration and libration can indeed significantly affect the calculated coupling. The ESID model was evaluated for a series of crystal dimer structures (vide infra) with both the B3LYP and PW91 functionals using a 6-31G** basis set. All EDH calculations were performed with the PW91 functional using the generalized gradient approximation (GGA) and a triple-ζ STO basis set with one polarization function on each atom (TZP basis) with the Amsterdam Density Functional code (ADF) [76–78]. Dimers along specific directions were extracted from the crystal structures and the electronic coupling $t^{H[L]}_{1,2}$ was evaluated as the matrix element $< \varphi^{H[L]}_1 | H | \varphi^{H[L]}_2 >$ (where $\varphi^{H[L]}_{1,2}$ are the localized HOMO and LUMO molecular orbitals).

Received: July 3, 2007
Revised: October 15, 2007

[1] F. Garnier, *Chem. Phys.* **1998**, *227*, 253.
[2] H. E. Katz, Z. N. Bao, S. L. Gilat, *Acc. Chem. Res.* **2001**, *34*, 359.
[3] A. Facchetti, M. Mushrush, M. H. Yoon, G. R. Hutchison, M. A. Ratner, T. J. Marks, *J. Am. Chem. Soc.* **2004**, *126*, 13859.
[4] A. Facchetti, M. H. Yoon, C. L. Stern, G. R. Hutchison, M. A. Ratner, T. J. Marks, *J. Am. Chem. Soc.* **2004**, *126*, 13480.
[5] M. J. Panzer, C. D. Frisbie, *Appl. Phys. Lett.* **2006**, *88*, 203504/1.
[6] H. Yan, M. H. Yoon, A. Facchetti, T. J. Marks, *Appl. Phys. Lett.* **2005**, *87*, 183501/1.
[7] C. W. Tang, S. A. Vanslyke, *Appl. Phys. Lett.* **1987**, *51*, 913.
[8] C. W. Tang, S. A. Vanslyke, C. H. Chen, *J. Appl. Phys.* **1989**, *65*, 3610.
[9] J. H. Burroughes, D. D. C. Bradley, A. R. Brown, R. N. Marks, K. Mackay, R. H. Friend, P. L. Burns, A. B. Holmes, *Nature* **1990**, *347*, 539.
[10] S. A. VanSlyke, C. H. Chen, C. W. Tang, *Appl. Phys. Lett.* **1996**, *69*, 2160.
[11] R. H. Friend, R. W. Gymer, A. B. Holmes, J. H. Burroughes, R. N. Marks, C. Taliani, D. D. C. Bradley, D. A. Dos Santos, J.-L. Brédas, M. Logdlund, W. R. Salaneck, *Nature* **1999**, *397*, 121.
[12] G. Malliaras, R. Friend, *Phys. Today* **2005**, *58*, 53.
[13] L. S. C. Pingree, M. T. Russell, T. J. Marks, M. C. Hersam, *J. Appl. Phys.* **2006**, *100*, 044502.
[14] J. Zaumseil, R. H. Friend, H. Sirringhaus, *Nat. Mater.* **2006**, *5*, 69.
[15] M. Granstrom, K. Petritsch, A. C. Arias, A. Lux, M. R. Andersson, R. H. Friend, *Nature* **1998**, *395*, 257.
[16] L. Ding, M. Jonforsen, L. S. Roman, M. R. Andersson, O. Inganas, *Synth. Met.* **2000**, *110*, 133.
[17] J. Roncali, *Chem. Soc. Rev.* **2005**, *34*, 483.
[18] H. E. Katz, *Chem. Mater.* **2004**, *16*, 4748.
[19] A. Dodabalapur, *Mater. Today* **2006**, *9*, 24.
[20] T. B. Singh, N. S. Sariciftci, *Annu. Rev. Mater. Res.* **2006**, *36*, 199.
[21] H. Sirringhaus, P. J. Brown, R. H. Friend, M. M. Nielsen, K. Bechgaard, B. M. W. Langeveld-Voss, A. J. H. Spiering, R. A. J. Janssen, E. W. Meijer, P. Herwig, D. M. de Leeuw, *Nature* **1999**, *401*, 685.
[22] J.-L. Brédas, D. Beljonne, V. Coropceanu, J. Cornil, *Chem. Rev.* **2004**, *104*, 4971.
[23] K. Hannewald, P. A. Bobbert, *Appl. Phys. Lett.* **2004**, *85*, 1535.
[24] R. A. Marcus, *J. Chem. Phys.* **1956**, *24*, 979.
[25] R. A. Marcus, *Can. J. Chem.* **1959**, *37*, 155.
[26] R. A. Marcus, *J. Phys. Chem.* **1963**, *67*, 853.
[27] P. F. Barbara, T. J. Meyer, M. A. Ratner, *J. Phys. Chem.* **1996**, *100*, 13148.
[28] I. V. Leontyev, A. V. Tovmash, M. V. Vener, I. V. Rostov, M. V. Basilevsky, *Chem. Phys.* **2005**, *319*, 4.
[29] J. R. Reimers, Z. L. Cai, N. S. Hush, *Chem. Phys.* **2005**, *319*, 39.
[30] M. V. Vener, A. V. Tovmash, I. V. Rostov, M. V. Basilevsky, *J. Phys. Chem. B* **2006**, *110*, 14950.
[31] A. A. Milischuk, D. V. Mayushov, M. D. Newton, *Chem. Phys.* **2006**, *324*, 172.
[32] S. R. Manjari, H. J. Kim, *J. Phys. Chem. B* **2006**, *110*, 494.
[33] K. Senthilkumar, F. C. Grozema, F. M. Bickelhaupt, L. D. A. Siebbeles, *J. Chem. Phys.* **2003**, *119*, 9809.
[34] K. Senthilkumar, F. C. Grozema, C. G. Guerra, F. M. Bickelhaupt, F. D. Lewis, Y. A. Berlin, M. A. Ratner, L. D. A. Siebbeles, *J. Am. Chem. Soc.* **2005**, *127*, 14894.
[35] E. F. Valeev, V. Coropceanu, D. A. da Silva Filho, S. Salman, J.-L. Brédas, *J. Am. Chem. Soc.* **2006**, *128*, 9882.
[36] V. Coropceanu, J. Cornil, D. A. da Silva Filho, Y. Olivier, R. Silbey, J.-L. Brédas, *Chem. Rev.* **2007**, *107*, 926.

[37] M. Pope, C. E. Swenberg, *Electronic Processes in Organic Crystals and Polymers*, 2nd ed., Oxford University Press, New York **1999**.
[38] F. Wurthner, *Angew. Chem. Int. Ed.* **2001**, *40*, 1037.
[39] D. B. Mitzi, C. D. Dimitrakopoulos, L. L. Kosbar, *Chem. Mater.* **2001**, *13*, 3728.
[40] A. Kraft, *ChemPhysChem* **2001**, *2*, 163.
[41] C. D. Dimitrakopoulos, P. R. L. Malenfant, *Adv. Mater.* **2002**, *14*, 99.
[42] A. Afzali, C. D. Dimitrakopoulos, T. L. Breen, *J. Am. Chem. Soc.* **2002**, *124*, 8812.
[43] S. A. Ponomarenko, S. Kirchmeyer, A. Elschner, B. H. Huisman, A. Karbach, D. Drechsler, *Adv. Funct. Mater.* **2003**, *13*, 591.
[44] Y. Kunugi, K. Takimiya, K. Yamane, K. Yamashita, Y. Aso, T. Otsubo, *Chem. Mater.* **2003**, *15*, 6.
[45] H. Meng, M. Bendikov, G. Mitchell, R. Helgeson, F. Wudl, Z. Bao, T. Siegrist, C. Kloc, C. H. Chen, *Adv. Mater.* **2003**, *15*, 1090.
[46] C. Videlot, J. Ackermann, P. Blanchard, J. M. Raimundo, P. Frere, M. Allain, R. de Bettignies, E. Levillain, J. Roncali, *Adv. Mater.* **2003**, *15*, 306.
[47] M. Halik, H. Klauk, U. Zschieschang, G. Schmid, S. Ponomarenko, S. Kirchmeyer, W. Weber, *Adv. Mater.* **2003**, *15*, 917.
[48] H. Sandberg, O. Henze, A. F. M. Kilbinger, H. Sirringhaus, W. J. Feast, R. H. Friend, *Synth. Met.* **2003**, *137*, 885.
[49] A. Facchetti, M. H. Yoon, C. L. Stern, H. E. Katz, T. J. Marks, *Angew. Chem. Int. Ed.* **2003**, *42*, 3900.
[50] M. H. Yoon, A. Facchetti, C. E. Stern, T. J. Marks, *J. Am. Chem. Soc.* **2006**, *128*, 5792.
[51] M. Mushrush, A. Facchetti, M. Lefenfeld, H. E. Katz, T. J. Marks, *J. Am. Chem. Soc.* **2003**, *125*, 9414.
[52] H. E. Katz, L. Torsi, A. Dodabalapur, *Chem. Mater.* **1995**, *7*, 2235.
[53] A. J. Lovinger, D. D. Davis, A. Dodabalapur, H. E. Katz, *Chem. Mater.* **1996**, *8*, 2836.
[54] W. J. Li, H. E. Katz, A. J. Lovinger, J. G. Laquindanum, *Chem. Mater.* **1999**, *11*, 458.
[55] F. S. Schoonbeek, J. H. van Esch, B. Wegewijs, D. B. A. Rep, M. P. de Haas, T. M. Klapwijk, R. M. Kellogg, B. L. Feringa, *Angew. Chem. Int. Ed.* **1999**, *38*, 1393.
[56] G. Horowitz, M. E. Hajlaoui, *Adv. Mater.* **2000**, *12*, 1046.
[57] R. C. Haddon, T. Siegrist, R. M. Fleming, P. M. Bridenbaugh, R. A. Laudise, *J. Mater. Chem.* **1995**, *5*, 1719.
[58] S. E. Koh, B. Delley, J. E. Medvedeva, A. Facchetti, A. J. Freeman, T. J. Marks, M. A. Ratner, *J. Phys. Chem. B* **2006**, *110*, 24361.
[59] S. R. Marder, C. B. Gorman, F. Meyers, J. W. Perry, G. Bourhill, J.-L. Brédas, B. M. Pierce, *Science* **1994**, *265*, 632.
[60] V. Coropceanu, M. Malagoli, D. A. da Silva Filho, N. E. Gruhn, T. G. Bill, J.-L. Brédas, *Phys. Rev. Lett.* **2002**, *89*, 275503.
[61] N. E. Gruhn, D. A. da Silva Filho, T. G. Bill, M. Malagoli, V. Coropceanu, A. Kahn, J.-L. Brédas, *J. Am. Chem. Soc.* **2002**, *124*, 7918.
[62] J.-L. Brédas, R. Silbey, D. S. Boudreaux, R. R. Chance, *J. Am. Chem. Soc.* **1983**, *105*, 6555.
[63] R. Cervini, X. C. Li, G. W. C. Spencer, A. B. Holmes, S. C. Moratti, R. H. Friend, *Synth. Met.* **1997**, *84*, 359.
[64] D. M. deLeeuw, M. M. J. Simenon, A. R. Brown, R. E. F. Einerhand, *Synth. Met.* **1997**, *87*, 53.
[65] G. P. Smestad, S. Spiekermann, J. Kowalik, C. D. Grant, A. M. Schwartzberg, J. Zhang, L. M. Tolbert, E. Moons, *Sol. Energy Mater. Sol. Cells* **2003**, *76*, 85.
[66] H. Li, J.-L. Brédas, C. Lennartz, *J. Chem. Phys.* **2007**, *126*, 164704.
[67] C. Kittel, *Introduction to Solid State Physics*, 7th ed., Wiley, New York **1996**.
[68] A. Burin, M. A. Ratner, in *Computational Materials Chemistry: Methods and Applications* (Eds: L. A. G. Curtiss, M. S. Gordon), Kluwer, Dordrecht, The Netherlands **2004**, pp. 308–367.
[69] J. Zaumseil, H. Sirringhaus, *Chem. Rev.* **2007**, *107*, 1296.
[70] A. D. Becke, *J. Chem. Phys.* **1993**, *98*, 5648.
[71] C. T. Lee, W. T. Yang, R. G. Parr, *Phys. Rev. B* **1988**, *37*, 785.
[72] J. P. Perdew, Y. Wang, *Phys. Rev. B* **1992**, *45*, 13244.
[73] W. A. Shapley, D. P. Chong, *Int. J. Quantum Chem.* **2001**, *81*, 34.
[74] J. Kong, C. A. White, A. I. Krylov, D. Sherrill, R. D. Adamson, T. R. Furlani, M. S. Lee, A. M. Lee, S. R. Gwaltney, T. R. Adams, C. Ochsenfeld, A. T. B. Gilbert, G. S. Kedziora, V. A. Rassolov, D. R. Maurice, N. Nair, Y. H. Shao, N. A. Besley, P. E. Maslen, J. P. Dombroski, H. Daschel, W. M. Zhang, P. P. Korambath, J. Baker, E. F. C. Byrd, T. Van Voorhis, M. Oumi, S. Hirata, C. P. Hsu, N. Ishikawa, J. Florian, A. Warshel, B. G. Johnson, P. M. W. Gill, M. Head-Gordon, J. A. Pople, *J. Comput. Chem.* **2000**, *21*, 1532.
[75] A. Troisi, *Adv. Mater.* **2007**, *19*, 2000.
[76] C. Fonseca Guerra, J. G. Snijders, G. te Velde, E. J. Baerends, *Theor. Chim. Acta* **1998**, *99*, 391.
[77] G. te Velde, F. M. Bickelhaupt, C. Fonseca Guerra, E. J. Baerends, J. G. Snijders, T. Ziegler, *J. Comput. Chem.* **2001**, *22*, 931.
[78] E. J. Baerends, J. Autschbach, A. Bérces, F. M. Bickelhaupt, C. Bo, P. M. Boerrigter, L. Cavallo, D. P. Chong, L. Deng, R. M. Dickson, D. E. Ellis, M. v. Faassen, L. Fan, T. H. Fischer, C. F. Guerra, S. J. A. v. Gisbergen, J. A. Groeneveld, O. V. Gritsenko, M. Grüning, F. E. Harris, P. v. d. Hoek, C. R. Jacob, H. Jacobsen, L. Jensen, G. v. Kessel, F. Kootstra, E. v. Lenthe, D. A. McCormack, A. Michalak, J. Neugebauer, V. P. Nicu, V. P. Osinga, S. Patchkovskii, P. H. T. Philipsen, D. Post, C. C. Pye, W. Ravenek, P. Ros, P. R. T. Schipper, G. Schreckenbach, J. G. Snijders, M. Solà, M. Swart, D. Swerhone, G. t. Velde, P. Vernooijs, L. Versluis, L. Visscher, O. Visser, F. Wang, T. A. Wesolowski, E. v. Wezenbeek, G. Wiesenekker, S. K. Wolff, T. K. Woo, A. L. Yakovlev, T. Ziegler, *ADF2007.01*, Vrije Universiteit, Amsterdam **2007**.